

# Squeeze Films Characteristics in the Poiseuille Flow

Enasy Abdullah<sup>1</sup>, Ali m Abdulameer<sup>2</sup>

<sup>1</sup>Department of Mathematic, Faculty of Education , Kufa University

<sup>2</sup>Department of Mathematic, Faculty of Computer Science & Mathematics, KufaUniversity

Email:inasy.abdullah@uokufa.edu.iq

Email:alim.khalefa@student.uokufa.edu.iq

## Article Info

Volume 83

Page Number: 14812 – 14822

Publication Issue:

March - April 2020

## Article History

Article Received: 24 July 2019

Revised: 12 September 2019

Accepted: 15 February 2020

Publication: 22 April 2020

## Abstract:

In this paper, introduced squeeze films characteristics in the poiseuille flow. Depended on The Reynolds equation for speed molecules and squeeze action is mathematically derived. The research focused on a study friction force between layers, center of pressure and rate of flow. It found increases speed molecules for first layers lead to increased friction force, rate of flow pressure and decreed center of pressure.

**Keywords:** Films, Poiseuille, Flow

---

## Nomenclature

h	Film thickness	x, y	Coordinates along the direction
B	Porosity of thin film	P	Pressure in thin film
U	Sliding motion	$\rho$	Density
V	Squeeze action	$\mu$	Viscosity of thin film
$U_s$	Infusion of molecules	$f_h$	Flexibility of the thin film
$h_m$	Minimum film thickness	R	Radius
W	Load carrying capacity	T	Time flow

## I INTRODUCTION

Thin films are described by thin layers of materials whose dimensions range from nanometres to several micrometres in thickness. They are added to the surface of the material in order to add properties that were not there before, such as durability, various loads, reducing friction and corrosion. This technology is used in the manufacture of semiconductors and in coatings [1]. They are exercised to memorize surfaces from wear, recover lubricity, improve attrition and chemical resistance, modify optical and electrical properties. Thin films deposition technology and the science have progressed rapidly in the direction of engineered thin film coatings have

surface engineering [2]. Plasmas are used more extensively. Accordingly, advanced thin film deposition processes have been developed and new technologies have been adapted to conventional deposition processes. The market and applications for thin film coating have also increased astronomically, particularly in the biomedical, display and energy fields. Thin films have distinct advantages on porosity materials [3]. A thin film is a structure whose dimensions are such that it has a substantially large surface to volume ratio. For example, while the structure may be macroscopically large in length and width, it may have a thickness that is only on the order of a micron or less. Thin films do not have to be

planer. The properties of such thin film structures are strongly influenced by the surface properties and may be very different from that of the same material in bulk form. The thin films may consist of a pure material, or a composite or a layered structure, and several of thin films may be present in a more complex device. Each thin film feature is dependent on the porosity process and can be modified and not all processes produce materials with the same porosity and permeability of thin layers. Therefore, we found each thin layers have different load carry capacity, time approach that transfer film thickness to minimum film thickness [4].

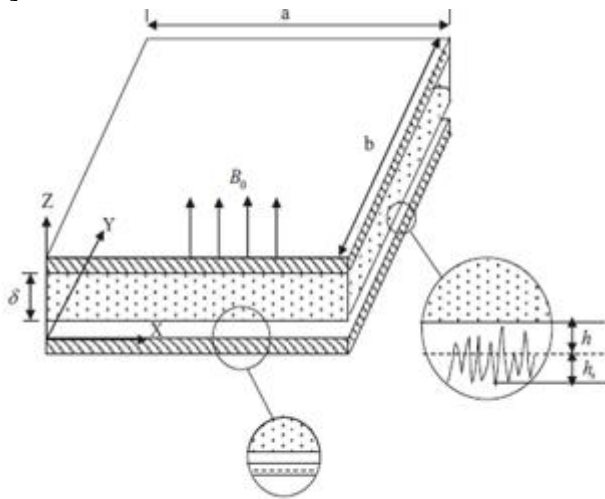


Figure 1: squeeze film geometry.

## II ANALYSIS

Based on Reynolds' equation, we can study the effect of some factors on the work of thin films, our study is on thin films in a case poiseuille flow when the surface fixed, now the Reynolds' equation is

$$\frac{\partial}{\partial x} \left( \frac{ph^3}{12\mu} \frac{dp}{dx} \right) + \frac{\partial}{\partial y} \left( \frac{ph^3}{12\mu} \frac{\partial p}{\partial y} \right) = \rho \frac{(U_a + U_b)}{2} \frac{\partial h}{\partial x} + (V_2 - V_1) + h \frac{\partial p}{\partial z} + F_h(1)$$

The first and two terms of the equation (1) are the poiseuille flow. The three is hydrodynamic and four terms squeeze film. The five is local expansion. In addition, the six is flexibility of the thin film, we need to satisfy the following

boundary condition, at the inlet  $P=0$  & At the outlet  $P = \frac{dp}{dx} = 0$ , the motion assumed as pure sliding and squeeze term and applying the last assumptions equation (1) becomes

$$\frac{d}{dx} \left( \frac{h^3}{\mu} \frac{dp}{dx} \right) = 6(U) \frac{dh}{dx} + 12(V) + 12F_h \quad (2)$$

Such that  $U=(U_a + U_b)$  &  $V=(V_2 - V_1)$ ,

Equation above can be integrated with consideration to x to give

$$\frac{h^3}{\mu} \frac{dp}{dx} = 6Uh + 12Vx + 12F_h x + A \quad (3)$$

Such that A is constant. So as to solve the Reynolds equation the integral A should be determined depended on boundary condition

$\frac{dp}{dx} = 0$  at  $h = h_0$ ,  $x = 0$ . Hence  $A =$

$-6Uh_0$  replace this into equation (3) gives

$$\frac{dp}{dx} = 6U\mu \frac{(h-h_0)}{h^3} + \frac{12V\mu x}{h^3} + 12 \frac{F_h \mu}{h^3} x \quad (4)$$

$$h = h_0 + \frac{x^2}{2R} \quad (5)$$

Where  $h_0$  film thickness & x is: coordinate

Now replace equation (5) in equation (4)

$$\frac{dp}{dx} = 6U\mu \frac{\left( \left( h_0 + \frac{x^2}{2R} \right) - \left( h_0 + \frac{x^2}{2R} \right) \right)}{\left( h_0 + \frac{x^2}{2R} \right)^3} + \frac{12V\mu}{\left( h_0 + \frac{x^2}{2R} \right)^3} x +$$

$$\frac{12F_h \mu}{\left( h_0 + \frac{x^2}{2R} \right)^3} x \quad (6)$$

$$\tan \beta = \frac{x}{\sqrt{2Rh_0}} \quad (7)$$

Replace equation (7) in equation (5) yields to

$$h = h_0 (1 + \tan^2 \beta) \quad (8)$$

$$h = h_0 \sec^2 \beta \quad (9)$$

Now distinguishing x and p with respect to  $\beta$  for equation (7)

$$\frac{\partial x}{\partial \beta} = \sqrt{2Rh_0} \sec^2 \beta \quad (10)$$

$$\partial p = \left[ 6U\mu \frac{(h_0 \sec^2 \beta - h_0 \sec^2 \beta)}{h_0^3 \sec^6 \beta} + \frac{12V\mu}{h_0^3 \sec^6 \beta} x + 12F_h \mu \frac{0.3 \sec^6 \beta x + 2Rh_0 \sec^2 \beta}{\partial \beta} \right] \quad (11)$$

### 2.1. Dimensionless friction force

To write modified Reynolds equation governing in the film pressure introducing the following dimensionless variables

$$\begin{aligned}
 P^* &= \frac{PH_0^2}{\mu U_o R} & h_0^* &= \frac{h_0}{H} & U^* &= \frac{U}{U_o} \\
 V &= \frac{V}{U_o} & \beta &= \frac{R}{h} & \bar{\beta} &= \frac{\bar{c}}{\alpha} \\
 F_h &= \frac{R}{h} & x^* &= \frac{x}{H} & U_s^* &= \frac{F_h}{U_o}
 \end{aligned}$$

The dimensionless Pressure equation become

$$P^* = \frac{6\sqrt{2}U^*}{(h_0^*)^2} \left[ \frac{13}{2} + \frac{\sin 2\beta}{4} \right] - \frac{6\sqrt{2}U^*}{(h_0^*)^2} [\sec^2 \bar{\beta} \left[ \frac{3}{8}\beta + \frac{\sin 2\beta}{4} + \frac{\sin 4\beta}{32} \right] + \frac{12V_2}{(h_0^*)^2} x^* (V^* - U_s^*) \left[ \frac{3}{8}\beta + \frac{1}{4}\sin 2\beta + 132\sin 4\beta \right] \quad (12)$$

Friction force between layers thin and molecules are a very important factor, to find friction force depended on shear stress action of surface films (smooth – roughness). Assume that Newtonian fluid and Newton law of viscosity be:

$$\tau = \mu \left( \frac{\partial u}{\partial z} \right) \quad [1]$$

(13)

Where  $\mu$  is dynamic viscosity and the term  $\left( \frac{du}{dz} \right)$

velocity gradient of  $z$  is obtained from the velocity distribution.

$$\frac{\partial u}{\partial z} = \frac{1}{\mu} \frac{\partial P}{\partial x} h_0^2 \left( Z - \frac{h}{2} \right) + \frac{UL}{2}$$

(14)

$$\mu \frac{\partial u}{\partial z} = \frac{\partial P}{\partial x} h_0^2 \left( Z - \frac{h}{2} \right) + \frac{UL}{2} \mu \quad (15)$$

Now introduce friction force law of surface:

$$F = \frac{1}{L} \int \mu \frac{\partial u}{\partial z} dx \quad (16)$$

$$FL = \int_0^\beta \left[ \frac{\partial P}{\partial x} h_0^2 \left( Z - \frac{h}{2} \right) + \frac{UL}{2} \mu \right] dx \quad (17)$$

Where (L) is length of thin film, the friction force is need on the two surfaces  $Z = h$  and  $Z = 0$ , writing  $F_h$  for the first and  $F_0$  for the second When  $Z = h$

$$FL = \int_0^\beta \left[ \frac{\partial P}{\partial x} h_0^2 \left( \frac{h}{2} \right) + \frac{UL}{2} \mu \right] dx \quad (18)$$

When  $Z = 0$

$$FL = \int_0^\beta \left[ -\frac{\partial P}{\partial x} h_0^2 \left( \frac{h}{2} \right) + \frac{UL}{2} \mu \right] dx$$

(19)

With positive sign for  $z = h$  and  $u = U$  and the negative sign for the film then  $Z = 0, U = 0$

$$FL = \int_0^\beta \frac{\partial P}{\partial x} h_0^2 \left( \frac{h}{2} \right) dx^* + \frac{UL}{2} \mu R dx^* \quad (20)$$

$$\frac{FL}{U\mu R} = \int_0^\beta \frac{\partial}{\partial x^*} \frac{Ph_0^3}{U\mu R} \frac{h_0^*}{2} dx^* + \frac{L^* h_0}{2} dx^*$$

(21)

$$F_h^* = \int_0^\beta \frac{\partial P^*}{\partial x^*} \frac{h_0^*}{2} dx^* + \frac{L^*}{2} dx^*$$

(22)

Derivative the dimensionless pressure hydrodynamic ( $p^*$ ) equation (12) we obtain

$$\frac{\partial p^*}{\partial x^*} = \frac{12\sqrt{2}}{h_0^{*2}} (V^* - U_s^*) \left[ \frac{3\beta}{8} + \frac{\sin 2\beta}{4} + \frac{\sin 4\beta}{32} \right]$$

(23)

Substitute equation (2.43) in equation (2.42), we get

$$F_h^* =$$

$$\frac{6\sqrt{2}}{h_0^{*2}} (V^* - U_s^*) \left[ \frac{3\beta}{8} + \frac{\sin 2\beta}{4} + \frac{\sin 4\beta}{32} \right] \int_0^\beta dx^* +$$

$$\frac{L^*}{2} \int_0^\beta dx^* \quad (24)$$

$$F_h^* = \frac{6\sqrt{2}}{h_0^{*2}} (V^* - U_s^*) \left[ \frac{3\beta^2}{8} + \frac{\beta \sin 2\beta}{4} + \frac{\beta \sin 4\beta}{32} \right] +$$

$$\frac{L^*}{2} \beta \quad (25)$$

In the same way we obtain force of friction when  $Z = 0$

$$F_0^* = \frac{6\sqrt{2}}{h_0^{*2}} (U_s^* - V^*) \left[ \frac{3\beta^2}{8} + \frac{\beta \sin 2\beta}{4} + \frac{\beta \sin 4\beta}{32} \right] +$$

$$\frac{L^*}{2} \beta \quad (26)$$

2.2. Dimensionless Center of Pressure

In general, the load carrying capacity is obtained by integration of the pressure distribution

$$W = 2\pi \int_0^L H_0 P \, dx \tag{27}$$

Introduce the non-dimensional load carrying capacity in consideration

$$W^* = \frac{12\pi\sqrt{2}U^*L}{(h_0^*)^2} \left( \frac{\beta}{2} + \frac{\sin 2\beta}{4} \right) + \frac{\sin 2\beta}{4} + \frac{\sin 4\beta}{23} + \frac{12\sqrt{2}L^2}{(h_0^*)^2} (V^* - U_s^*) \left( \frac{3\beta}{8} + \frac{\sin 2\beta}{4} + \frac{\sin 4\beta}{32} \right) \tag{30}$$

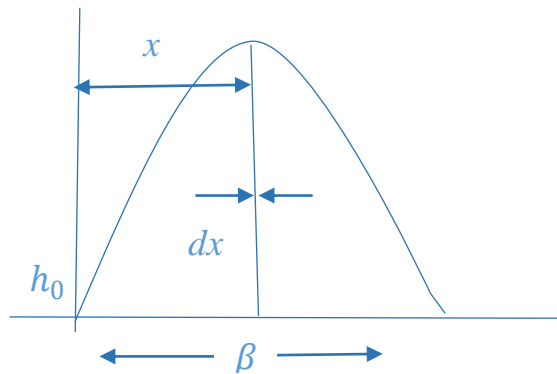


Figure 2: Center of pressure

$$W^* = \frac{W}{\mu U_0 R} \tag{28}$$

Replace equation (28) inside (27) and we integrate dimensionless pressure with assessment to the dimensionless x and thus we get

$$W^* = 2\pi \int_0^L P^* \, dx^* \tag{29}$$

$$\frac{12\pi\sqrt{2}U^*L}{(h_0^*)^2} \sec^2 \bar{\beta} \left( \frac{3\beta}{8} + U_s^* \left( \frac{3\beta}{8} + \frac{\sin 2\beta}{4} + \frac{\sin 4\beta}{32} \right) \right)$$

The location of the center of pressure  $x_{cp}$  indicates the position at which the resulting force is acting. The expression for calculating the location is

$$W_{xcp} = \frac{1}{\Omega} \int_0^L P x \, dx \tag{31}$$

Where  $\Omega$  is radial clearance

Substituting dimensionless distance ( $x^* = \frac{x}{L}$ ) in equation (31) yields to

$$W_{xcp}^* = \frac{3\sqrt{2}U^*L^2}{h_0^{*2}} \left( \frac{\beta}{2} + \frac{\sin 2\beta}{4} \right) - \frac{3\sqrt{2}U^*L^2}{h_0^{*2}} \sec^2 \bar{\beta} \left( \frac{3\beta}{8} + \frac{\sin 2\beta}{4} + \frac{\sin 4\beta}{32} \right) + \frac{4\sqrt{2}L^3}{h_0^{*2}} (V^* - U_s^*) \left( \frac{3\beta}{8} + \frac{\sin 2\beta}{4} + \frac{\sin 4\beta}{32} \right) \tag{35}$$

Introduce the formulacenter of pressure equation ( $x_{cp}$ )

$$x_{cp} = \frac{W^*}{W_{xcp}^*} \tag{36}$$

After that divide the load carrying capacity represent in equation (30) on result of integration of the equation (35). Therefore, the center of pressure can be written as

$$W_{xcp} \Omega = \int_0^L H^2 p x^* \, dx^* \tag{32}$$

$$\frac{W_{xcp} \Omega}{\mu UR} = \int_0^L \frac{L^2 P}{\mu UR} x^* \, dx^* \tag{33}$$

$$\frac{W_{xcp} \Omega}{\mu UR} = \int_0^L p^* x^* \, dx^* \tag{34}$$

Substituting pressure hydrodynamic equation (12) in equation (34) yields to

$$x_{cp} = \frac{\frac{12\sqrt{2}\pi L U^* \left(\frac{\beta}{2} + \frac{\sin 2\beta}{4}\right)}{h_0^{*2}} - \frac{12\sqrt{2}L \sec^2 \beta \left(\frac{3\beta}{8} + \frac{\sin 2\beta}{4} + \frac{\sin 4\beta}{32}\right)}{h_0^{*2}} + \frac{12\sqrt{2}L^2 \pi (V^* - U_s^*) \left(\frac{3\beta}{8} + \frac{\sin 2\beta}{4} + \frac{\sin 4\beta}{32}\right)}{h_0^{*2}}}{\frac{3\sqrt{2}\pi L^2 U^* \left(\frac{\beta}{2} + \frac{\sin 2\beta}{4}\right)}{h_0^{*2}} - \frac{3\sqrt{2}L^2 \sec^2 \beta \left(\frac{3\beta}{8} + \frac{\sin 2\beta}{4} + \frac{\sin 4\beta}{32}\right)}{h_0^{*2}} + \frac{4\sqrt{2}L^4 \pi (V^* - U_s^*) \left(\frac{3\beta}{8} + \frac{\sin 2\beta}{4} + \frac{\sin 4\beta}{32}\right)}{h_0^{*2}}} \quad (37)$$

### 2.3. Dimensionless Flow rate

Flow defined as the quantity of fluid (gas and liquid) that passes a point per unit time. A simple equation to represent this is

$$Q_x = \frac{\Omega}{t} \int_0^h U dz \quad (38)$$

$$\left\{ U = \frac{1}{2\mu V_{inst}} \frac{\partial P}{\partial x} (Z^2 - Zh) + (U_h - U_0) \frac{Z}{h} \right\} \quad (39)$$

Where  $V_{inst}$  : instantaneous velocity, substitute equation (39) in equation (38), we get

$$Q_x = \frac{\Omega}{t} \int_0^h \frac{1}{2\mu V_{inst}} \frac{\partial P}{\partial x} (Z^2 - Zh) + (U_h - U_0) \frac{Z}{h} dz \quad (40)$$

$$h^* = \frac{h}{L}, x^* = \frac{x}{R}, z^* = \frac{z}{L}, Q_x^* = Q_x \frac{t}{\Omega R} \quad (41)$$

Now, by substitution equation (41) into equation (40), we obtain on dimensionless flow rate ( $Q_x^*$ ).

$$Q_x^* = \int_0^h \frac{\partial p^*}{2\partial x^*} (-Z^{*2} + h^* Z^*) dz^* + (U_h - U_0) \frac{h^*}{2} \quad (42)$$

$$Q_x^* = \frac{1}{2} \frac{\partial p^*}{\partial x^*} \left[ \frac{h^{*3}}{6} \right] + (U_h - U_0) \frac{h^*}{2} \quad (43)$$

From equation (23) and substitute in equation (43), we get

$$Q_x^* = \sqrt{2} h^{*2} (V^* - U_s^*) \left( \frac{3\beta}{8} + \frac{\sin 2\beta}{4} + \frac{\sin 4\beta}{32} \right) + (U_h - U_0) \frac{h^*}{2} \quad (44)$$

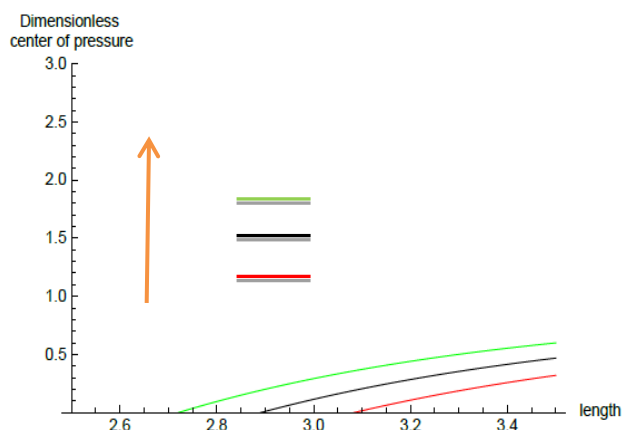


Figure (3): The variation of dimensionless center of pressure ( $x_{cp}^*$ ) of with length (L) for various dimensionless speed of molecular ( $U_s^*$ ).

### III RESULT AND DISCUSSION

Based on the Reynolds equation, this chapter discusses effective of properties of thin film in poiseuille flow.

#### 3.1. Center of pressure

The dimensionless center of pressure ( $x_{cp}^*$ ) as a function of length (L) for different values of the speed of molecules parameters ( $U_s^*$ ) is shown in figure (3), it is observed that increasing the center of pressure for thin films lead to decreases values of the speed of molecules ( $U_s^*$ ), explained that energy absorption increases with the increases motion of the molecules between layers of thin films and as a result decreasing the center of pressure, and relationship center of pressure with the difference of the speed of the molecules shown in the table (1). The different dimensionless center of pressure as a function of the length for different value of film thickness ( $h^*$ ) is seen in figure (4). It is shown that the center of pressure of increases with decreases values of ( $h^*_0$ ), It is shown that the center of pressure of increases with decreases values of

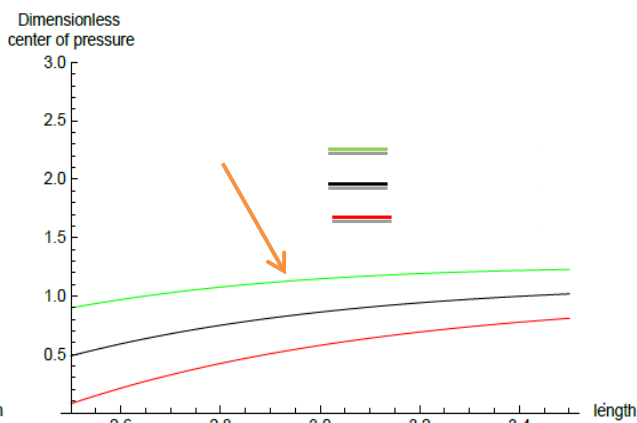


Figure (4): The variation of dimensionless center of pressure ( $x_{cp}^*$ ) of with length (L) for various dimensionless film thickness ( $h_0^*$ ).

$(h^*_0)$ . The dimensionless center of pressure ( $x_{cp}^*$ ) as a function of length of layers ( $L$ ) for different values of squeeze action parameters ( $V^*$ ) is shown in figure (5). It is shown that the center of pressure increases with increasing values squeeze action ( $V^*$ ), clear that external force generated hydrodynamic pressure as previously explained in analysis of pressure, physically with increasing squeeze action between layers become movement of particles low and center of pressure high. The dimensionless center of pressure ( $x_{cp}^*$ ) as a function of length of layers ( $L$ ) for different values of porosity parameters ( $\beta$ ) is shown in figure (6). It has shown that the center of pressure increases with decreasing values of porosity ( $\beta$ ). When

center of pressure increasing then volume of porosity on layers shrinks and this contraction varies from layer to layer. The different dimensionless center of pressure as a function of the length of layers for different values sliding motion ( $U^*$ ) is seen figure (7). Sliding motion between layers occurs interaction between particular fluid and members that it generated couple stress as a result curved pressure are high so center of pressure. The effect of the length of layers parameter ( $L$ ) on the variation of center of pressure ( $x_{cp}^*$ ) with porosity ( $\beta$ ) is shown in figure (8). It is shown that the center of pressure of increases with increasing values of length of layers of thin films ( $L$ ).

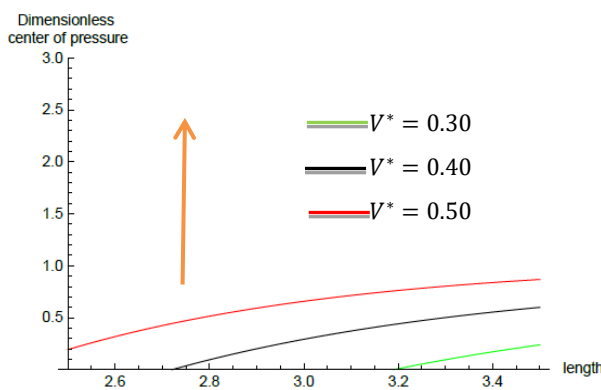


Figure (5): The variation of dimensionless center of pressure ( $x_{cp}^*$ ) of with length ( $L$ ) for various dimensionless squeeze action

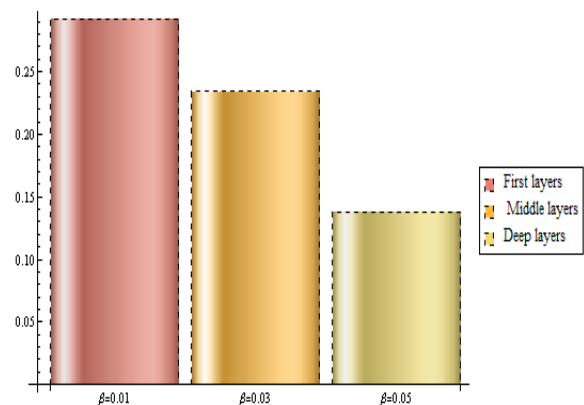


Figure (6): The variation of dimensionless center of pressure ( $x_{cp}^*$ ) of with length ( $L$ ) for various porosity ( $\beta$ ).

### 3.2 friction force

Illustrates dimensionless the friction force

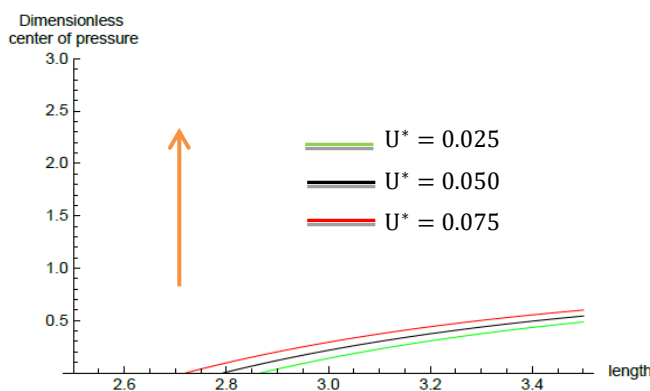


Figure (7): The variation of dimensionless center of pressure ( $x_{cp}^*$ ) of with length ( $L$ ) for various dimensionless sliding motion ( $U^*$ ).

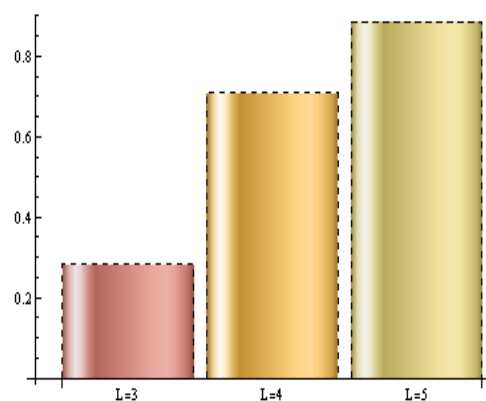
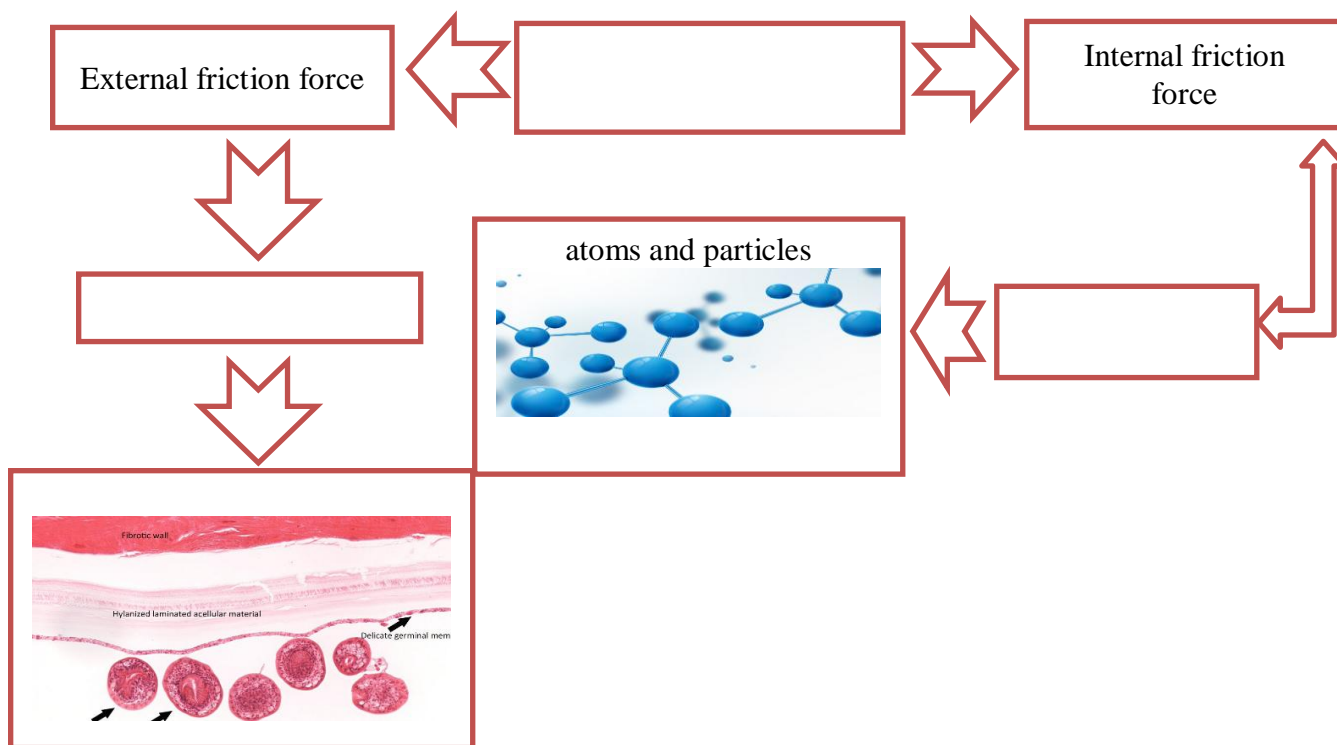


Figure (8): The variation of dimensionless center of pressure ( $x_{cp}^*$ ) of with Porosity ( $\beta$ ) for various Length ( $L$ ).



among thin of layers that consisting of atoms and molecules. The different dimensionless friction force as a function of the length for different value different speed of molecular ( $U_s$ ) be seen in figure (10). Friction strength between objects due to bumps or gaps between surfaces. When the velocity of the particles is high, the porosity of the

membrane surfaces is also high and as a result the friction strength is high, the opposite occurs when the speed of the particles is low. As well as each film of layers different speed of molecules since hydrodynamic pressure, therefore friction force in one- film become very high then it starts to decrease with the other layers. See table (2)



The different dimensionless friction force as a function of the length for different value of thin layers is seen in figure (11). When layers of film appears thickness this mean that pressure and load carrying low so friction force between layers this case it found in final layers while appears thin film since the high pressure these layers are exposed first layers which results in higher friction between the layers. The different dimensionless friction force as a function of the length for different squeeze action between layers is seen in figure (12). When squeeze action increasing in the first layers turns up thickness film to thin film as a result friction force increase an estimated rate of increase 90% while in final layers squeeze action

less and on it estimated rate friction force with 65%. The different dimensionless friction force as a function of the length for different porosity is seen in figure (13). The protrusions on the surfaces of the membranes vary with the hydrodynamic pressure. The higher the pressure, the less protrusions and the less friction with them. at  $\beta = 0.05$  estimated rate friction force with 70%. When  $\beta = 0.01$  estimated rate friction force with 5%. The different dimensionless friction force as a function of the speed of molecular different length is seen in figure (14). When length increasing distribution pressure less this lead to low friction force compared to shorter surface.

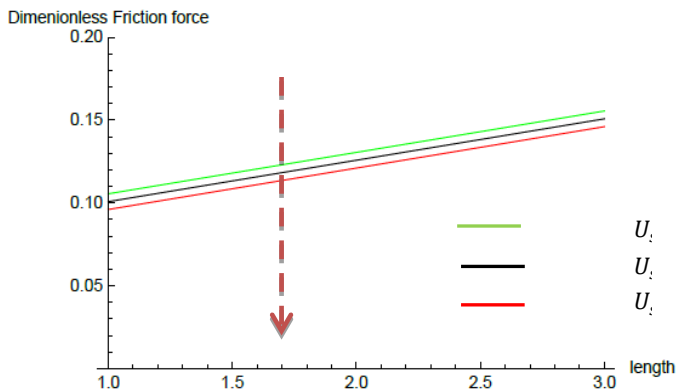


Figure (10): The variation of dimensionless Friction force ( $F^*$ ) of with Length ( $l^*$ ) for different dimensionless speed of molecular ( $U_s^*$ )

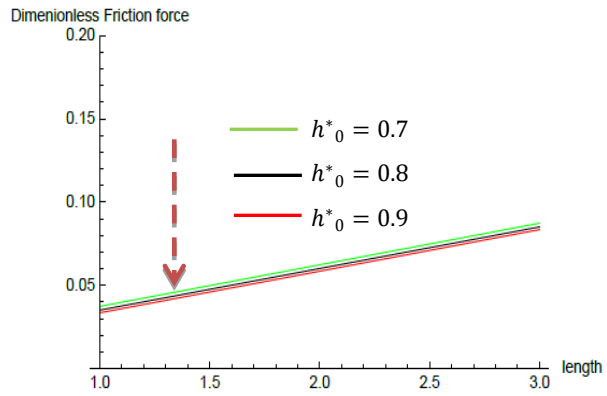


Figure (11): The variation of dimensionless Friction force ( $F^*$ ) of with Length ( $l^*$ ) for different dimensionless film thickness ( $h^*$ )

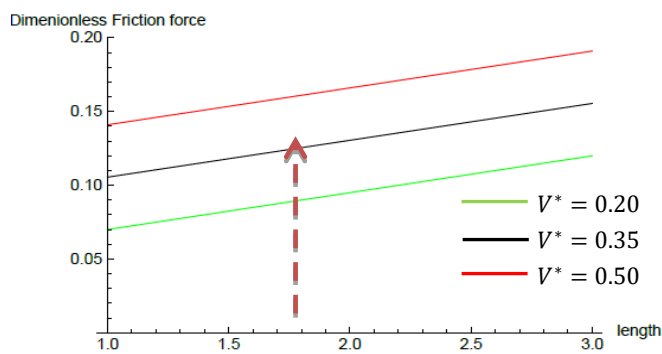


Figure (12): The variation of dimensionless Friction force ( $F^*$ ) of with Length ( $l^*$ ) for different dimensionless squeeze action ( $v^*$ )

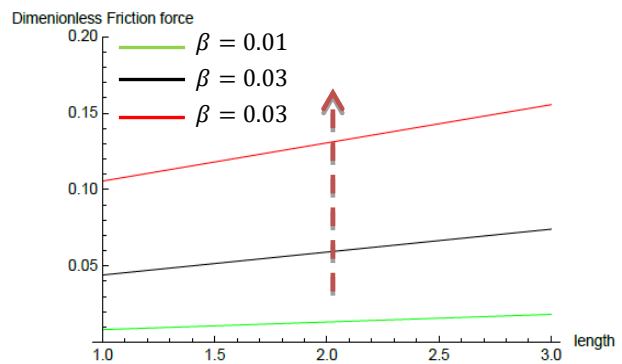


Figure (13): The variation of dimensionless Friction force ( $F^*$ ) of with Length ( $l^*$ ) for different porosity ( $\beta$ ).

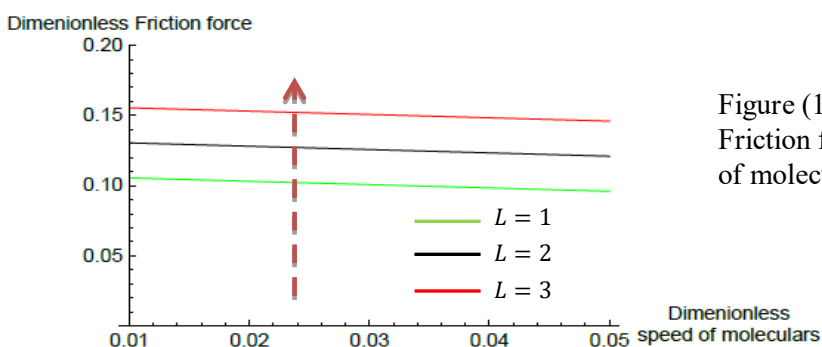


Figure (14): The variation of dimensionless Friction force ( $F^*$ ) of with dimensionless speed of molecular ( $U_s^*$ ) for different Length ( $L$ )



### 3.3 Flow rate

The dimensionless flow rate ( $Q_x^*$ ) as a function of dimensionless film thickness ( $h^*$ ) for different values of the dimensionless speed of particles parameters ( $U_s^*$ ) is shown in figure (15). After applying equation (44) in the computer program (Mathematica 11) noticed that the increasing of speed of particles decreases of flow rate, explained that the increases speed of particles leads to decreases pressure and this leads to increases sliding motion between layers and this mean increases flow rate. The dimensionless flow rate ( $Q_x^*$ ) as a function of porosity ( $\beta$ ) for different values of the dimensionless film thickness parameters ( $h^*$ ) is shown in figure (16). After applying equation (44) in the computer program (Mathematica 11) noticed that the increasing of film thickness ( $h^*$ ) increases of flow rate, explained that the increases film thickness leads to decreases pressure and this leads to increases sliding motion between layers and this mean increases flow rate. The dimensionless flow rate ( $Q_x^*$ ) as a function of dimensionless film thickness ( $h^*$ ) for different values of squeeze action ( $V^*$ ) is shown in figure (17). After applying

equation (44) in the computer program (Mathematica 11) noticed that increasing of squeeze action ( $V^*$ ) increases flow rate. The dimensionless flow rate ( $Q_x^*$ ) as a function of dimensionless film thickness ( $h^*$ ) for different values of the porosity parameters ( $\beta$ ) is shown in figure (18). After applying equation (44) in the computer program (Mathematica 11) noticed that the increasing of porosity increases of flow rate, explained that the increases porosity leads to decreases pressure and this leads to increases sliding motion between layers and this mean increases flow rate.

The dimensionless flow rate ( $Q_x^*$ ) as a function of dimensionless film thickness ( $h^*$ ) for different values of the sliding motion between layers parameters ( $U_h^*$ ) is shown in figure (19). After applying equation (44) in the computer program (Mathematica 11) noticed that the increasing of sliding motion between layers increases of flow rate, explained that the increasing of sliding motion between layers leads to increasing distance between the layers and this implies increasing film thickness.

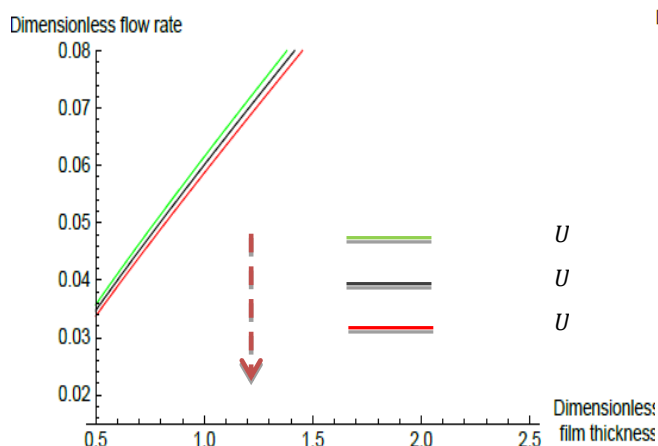


**Figure (15):** The variation of dimensionless Flow rate ( $Q_x^*$ ) of with dimensionless film thickness ( $h^*$ ) for different dimensionless speed of molecules ( $U_s^*$ ).

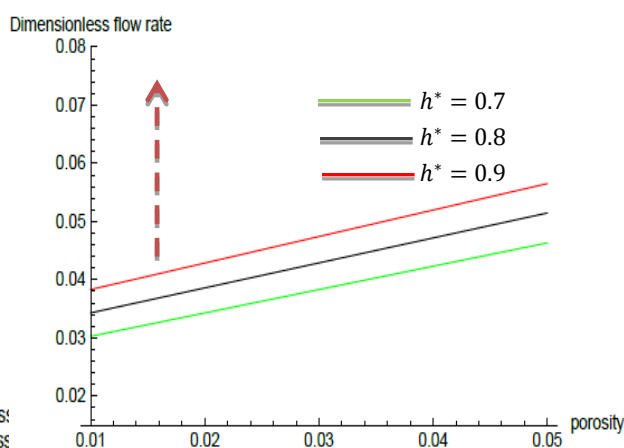


**Figure (16):** The variation of dimensionless Flow rate ( $Q_x^*$ ) of with porosity ( $\beta$ ) for different film thickness ( $h^*$ ).

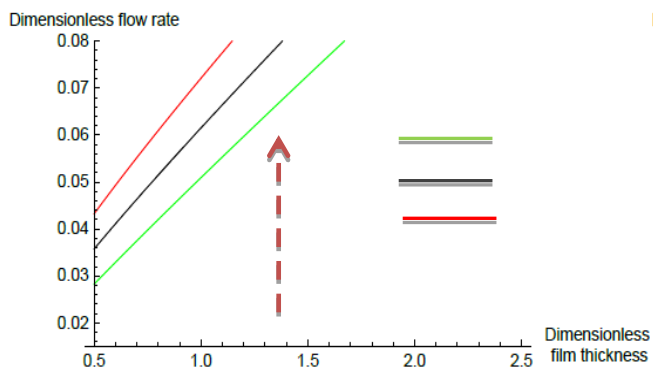


**Figure (17):** The variation of dimensionless Flow rate ( $Q_x^*$ ) of with dimensionless film thickness ( $h^*$ ) for different dimensionless squeeze action

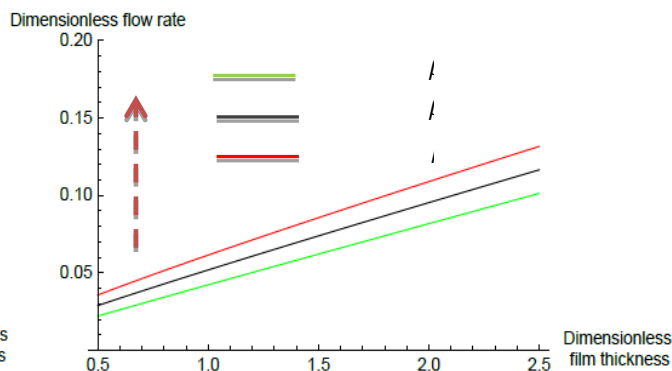


**Figure (18):** The variation of dimensionless Flow rate ( $Q_x^*$ ) of with dimensionless film thickness ( $h^*$ ) for different porosity ( $\beta$ )

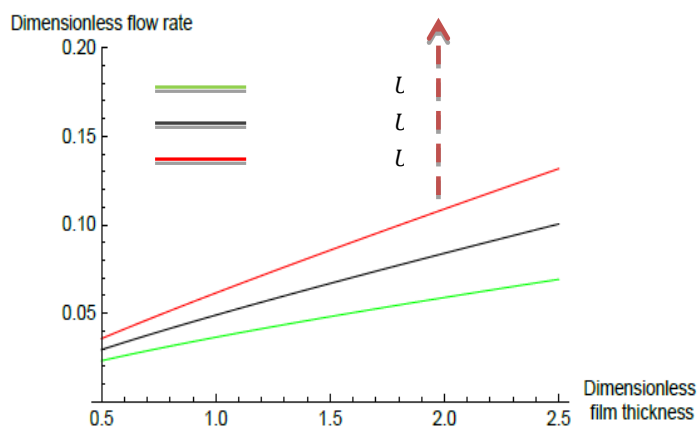


**Figure (19):** The variation of dimensionless Flow rate ( $Q_x^*$ ) of with dimensionless film thickness ( $h^*$ ) for different dimensionless sliding motion ( $U_h^*$ ).

Table 1

The different between dimensionless center of pressure ( $x_{cp}^*$ ) with the dimensionless pressure ( $P^*$ ) for different the speed of molecules parameters ( $U_s^*$ )

The speed of molecules ( $U_s^*$ )	The dimensionless pressure ( $P^*$ )	The dimensionless center of pressure ( $x_{cp}^*$ )
0.01	4.83314	0.59955
0.02	4.66343	0.536121
0.03	4.44372	0.468727
0.04	4.3240	0.396986
0.05	4.2910	0.320462

Table 2  
Relationship between friction force and speed of molecular with different layers of films

One - film		Two-film		Three- film	
$U_s$	$F^*$	$U_s$	$F^*$	$U_s$	$F^*$
0.05	0.06497	0.05	0.05288	0.05	0.051339
0.04	0.06557	0.04	0.05299	0.04	0.051393
0.03	0.06617	0.03	0.05311	0.03	0.051446
0.02	0.066772	0.02	0.05322	0.02	0.051500
0.01	0.067371	0.01	0.05334	0.01	0.05155
0	0.06797	0	0.05345	0	0.05160

#### IV CONCLUSION

1. The increasing speed of the particles results in absorption of energy low center of pressure.
2. High squeeze action and sliding motion leading to an increase in the flow of liquid responsible for generating center of pressure.
3. High center of pressure corresponds to the longest thin films, so high thickness film between layers makes the liquid flow less and center of pressure.
4. The increased speed of particle results in lower pressure and increased friction between layers so higher squeeze action due to external force increases friction, the longer films also have the same result.
5. The thickness of the high film represents the protection of the layers from friction while increased porosity of layers leads increased friction.
6. Increased sliding motion and squeeze action are consistent with increased flow rate.
7. When the thickness of the film and porosity are high the flow rate increases.
8. Speed of the particles have major effect on decreasing flow rate.

#### V REFERENCE

- [1] G.M.Deheri, (2011) " Load carrying capacity and time height relation for squeeze film between rough porous rectangular plates" annals of faculty engineering hunedoara –International journal of engineering pp.33-38.
- [2] R.F.Lu ,(2007) "A theoretical study of combined effects of non-Newtonian rheology and viscosity – pressure dependence in sphere- plate squeeze film system "Science direct. Tribology International.Vol.40, pp.125-131.
- [3] E.Y. Abdullah ,(2019) " Analysis squeeze film characteristics in synovial hip joint by using mathematical model" IOP Conference series: Materials science and engineering pp.1-14.
- [4] M.Scherge , and S.N .Gorb (2019) "Biological Micro-and Nano-tribology :Natures solutions"Germany :Spring –Verlag berlin Heidelberg.2001.
- [5] E.Y. Abdullah and A.A. Aladilee ,(2019) "To calculate effective particle of long chain polymer on velocity and flow rate using mathematical model" Sci.Int.(Lahore),31 (5),pp.739-744.
- [6] N.B. Naduvinamani, S.T. Fathima, and S. Jamal, (2010) "Effect of roughness on hydromagnetic squeeze films between porous rectangular plates" Science direct. Tribology International.Vol.43, pp.2145-2151